Zahn, R., Comas, M.C., and Klaus, A. (Eds.), 1999
Proceedings of the Ocean Drilling Program, Scientific Results, Vol. 161

39. PLANKTONIC $\delta^{18}O$ AND $U^{k'}_{37}$ TEMPERATURE ESTIMATES FROM ORGANIC-RICH SEDIMENTS AT SITES 974 AND 975, TYRRHENIAN SEA AND BALEARIC RISE[1]

Heidi Doose,[2,3] Rainer Zahn,[2] Stefano Bernasconi,[4] Milena Pika-Biolzi,[4,5] Anne Murat,[6] Catherine Pierre,[7] and Paul Belanger[8]

ABSTRACT

Sapropels at Sites 974 and 975 as well as sediment samples from immediately below and above sapropels were analyzed for alkenone concentrations. Paleo–sea-surface temperatures (SSTs) were inferred from the $U^{k'}_{37}$ unsaturation index in Pleistocene sapropel sequences. These SST estimates vary between 13° and 25°C. The upper range of SST estimates is distinctly warmer than modern mean annual SST at both sites and closely groups around the modern summer SST. The cold end of the inferred SST range is still warmer than the mean glacial winter SSTs from the Climate Long-Range Investigation Mapping and Prediction Project (CLIMAP) planktonic foraminifer census counts (Thiede, 1978). We infer, therefore, that sapropel formation at both sites was coeval with warm climates. Using planktonic $\delta^{18}O$ and $U^{k'}_{37}$ SST estimates as input into an oxygen isotope paleotemperature equation, we can deduce seawater $\delta^{18}O$ which, in turn, we can use to infer the paleosalinity for two Pleistocene sapropels at Site 975. These paleosalinity estimates are between 32 and 34, considerably lower than the modern salinity of 37.5 at this location. If we use more negative freshwater δ_w values in the equation, then the salinity offsets are reduced by 2–4 units. Depleted salinities, whatever their true values might have been, in conjunction with increased SSTs, imply that sapropel formation in the western Mediterranean occurred during warm and moist climates. This agrees with the idea that sapropel formation in the eastern Mediterranean is a result of enhanced northern hemisphere insolation. Whether or not climatic forcing caused similar marine environmental responses (such as enhanced biological productivity and/or reduced deep-water circulation) in both the eastern and western Mediterranean remains to be determined.

INTRODUCTION

The occurrence of organic-rich sediments (sapropels) is a common feature of sediment sequences throughout Pleistocene, Pliocene, and Miocene times of the eastern Mediterranean (e.g., Kullenberg, 1952; Olausson, 1961; Cita et al., 1977; Vergnaud-Grazzini et al., 1977; Williams and Thunell, 1979; Rossignol-Strick et al., 1982; Fontugne and Calvert, 1992; and others). During Ocean Drilling Program (ODP) Leg 107, distinct sapropel intervals of upper Pliocene to Pleistocene age were recovered in the Tyrrhenian Sea. During ODP Leg 161, sapropels and organic-rich layers have been discovered in the Balearic and Alboran Seas (Murat, Chap. 41, this volume; de Kaenel et al., Chap. 13, this volume) which makes a re-evaluation of possible mechanisms of sapropel formation necessary.

Sapropels are defined to be discrete finely laminated (Nesteroff, 1973) layers, more than 1 cm thick, and containing more than 2 wt% organic carbon (Kidd et al., 1978). Hilgen (1991) proposed a concept that explains the formation of sapropels in view of orbitally driven variations in northern hemisphere insolation. According to this concept, sapropels correlate with periods of minimum orbital precession, which are coeval with maximum northern hemisphere insolation. This concept was later confirmed and confined by other workers (e.g., Lourens et al., 1996). Sapropels in this conceptual model are defined as sedimentary units containing higher than background organic carbon concentrations. For Leg 161 we followed this definition to determine the occurrence of sapropels or organic-rich layers (ORL; Murat, Chap. 41, this volume) at the western Mediterranean drill sites.

To determine environmental conditions during sapropel formation requires reconstruction of hydrographic parameters: ambient surface-water paleotemperature and paleosalinity before, during, and after sapropel formation. As demonstrated by Rostek et al. (1993), sea-surface temperature (SST) and paleosalinity can be estimated by using the combined planktonic foraminiferal oxygen isotope and alkenone $U^{k'}_{37}$ signals. Reliable application of this strategy, however, requires knowledge about growth season and depth habitats for both planktonic foraminifers used for isotope analysis and of phytoplankton species used for alkenone measurements. For instance, we chose planktonic foraminifer *Globigerina bulloides* for isotope analysis, which occurs commonly in glacial and interglacial sections of sediment cores in the western Mediterranean Sea. This species has been shown to preferentially grow in spring (April–May; Kallel et al., 1997) at water depths between 50 and 200 m (Hemleben and Spindler, 1983). The primary alkenone-producing prymnesiophyte *Emiliania huxleyi*, on the other hand, preferentially dwells in the upper 20–50 m of the mixed layer and blooms from March to November (Knappertsbusch, 1993). Therefore, $\delta^{18}O$ derived from *G. bulloides* and SST inferred from $U^{k'}_{37}$ index of *E. huxleyi* both combine hydrographic signals from different seasons and different water depths. This does limit the accuracy of estimated paleosalinity, which must be kept in mind when reconstructing ocean conditions during discrete time intervals. Furthermore, *E. huxleyi,* which is believed to be the main producer of alkenones in the modern ocean (Volkman et al., 1980; Marlowe et al., 1984) and has been used for calibration of the alkenone paleotemperature equation (Prahl and Wakeham, 1987; Prahl et al., 1988; Ternois et al., 1997), first appears in the geologic record at (268 ka; Thierstein et al., 1977). For earlier Pleistocene periods, alkenones most probably were derived from the prymnesiophyte genus *Gephyrocapsa* (Marlowe et al., 1990), which, according to Volkman et al. (1995) shows a temperature sensitive $U^{k'}_{37}$ pattern similar to that of *E. huxleyi.* Whereas use of the $U^{k'}_{37}$ index to infer

[1]Zahn, R., Comas, M.C., and Klaus, A. (Eds.), 1999. *Proc. ODP, Sci. Results,* 161: College Station, TX (Ocean Drilling Program).

[2]GEOMAR Research Center for Marine Geosciences, Wischhofstrasse 1-3, D-24148 Kiel, Federal Republic of Germany.

[3]Present address: Bundesanstalt fuer Geowissenschaften und Rohstoffe Postfach 510153, 30631 Hannover, Federal Republic of Germany. doose@bgr.de

[4]Geologisches Institut, ETH-Zentrum, 8092 Zürich, Switzerland.

[5]Present address: Dipartimento di Scienze della Terra, Università degli Studi di Parma, Viale delle Scienze 78, 43100 Parma, Italy.

[6]INTECHMER, BP 324, Cherbourg Cedex, France.

[7]Université Pierre et Marie Curie, Laboratoire d'Océanographie Dynamique et de Climatologie, 4 Place de Jussieu, Case 100, F-75252 Paris Cedex 05, France.

[8]Department of Geological Sciences, University of Oregon, Eugene, OR 97403-1272, U.S.A. (Present address: 4429 Valerie St., Bellaire, TX 77401-5626, U.S.A.)

SST is thus not well constrained for the period before 268 ka, it can still be used to indicate general trends of SST changes.

Postdepositional oxidation of organic carbon poses additional limits on the use of $U^{k'}_{37}$ indices as SST indicators. Oxidation of organic matter has been demonstrated to affect the distribution of long-chain alkenones by preferential degradation of $C_{37:3}$ alkenones relative to $C_{37:2}$ alkenones (Ficken and Farrimond, 1995; Flügge, 1997; Hoefs et al., 1998). If concentrations of $C_{37:2}$ alkenones are high, as in the Madeira Abyssal Plain turbidites, degradation does not change the $U^{k'}_{37}$ index significantly across the redox boundary (Hoefs et al., 1998). $C_{37:3}$ alkenone concentrations are expected to be low in sediments from the Mediterranean because this compound tends to be depleted relative to $C_{37:2}$ alkenones in warm conditions. In such cases, the $U^{k'}_{37}$ index is largely determined by the abundance of $C_{37:2}$ alkenones. Therefore, preferential degradation of $C_{37:3}$ alkenones are of only minor importance for the $U^{k'}_{37}$ index.

In this study we use the $U^{k'}_{37}$ index at Sites 974 and 975 to reconstruct SST during periods of sapropel formation. To further evaluate hydrographic conditions we use planktonic $\delta^{18}O$ in combination with the $U^{k'}_{37}$-SST estimates to infer paleosalinity during these events.

Site Location and Oceanographic Setting

Site 975 is located on the South Balearic Margin between Mallorca and Menorca and the South-Balearic-Algerian-Basin. Characteristic circulation features are the Algerian Current and recirculated water that consists of water masses from the Balearic Sea. The Algerian Current is characterized by the occurrence of meso-scale anticyclonic eddies (diameter ≈100 km) that slowly move along the current axis (Deschamps et al., 1984). The presence of eddies force the Atlantic inflow (Modified Atlantic Water [MAW]) along a flow path close to the coast until near 0°E, where upon it gradually moves more offshore. Eddies developing near the coast generate upwelling cells that are biologically productive and are advected away from the coast (Arnone and La Violette, 1986). The hydrography of the Algerian Basin is largely defined by the dominance of Atlantic waters and, as such, constitutes a throughflow zone of Atlantic water moving east and north, thereby maintaining a reservoir of Atlantic water (Millot, 1987). The North Balearic front is defined as the northern boundary of this reservoir and closely delineates the extent of the Atlantic layer. Site 975 is within the MAW reservoir south of the Balearic Front.

Site 974 is also influenced by MAW, of which one-third is circulated by the Algerian current into the Tyrrhenian Sea. The Tyrrhenian Sea has two connections to the open Mediterranean, the Corsica Channel (sill depth about 350 m) to the north and the Sardinia Channel (sill depth about 2000 m) to the south, that enable an advection of water masses from the entire western Mediterranean (Astraldi and Gasparini, 1995). Surface waters at Site 974 are further influenced by two seasonally variable gyres. During winter and spring, a cyclonic eddy develops northeast of Corsica, and an anticyclonic eddy develops south off Sardinia. In summer and fall, the northern gyre becomes dominant, and the southern gyre moves further to the south, responding to an intensification of the northern gyre. This gyre circulation is stimulated by annually prevailing west winds in the Tyrrhenian Sea that also promote coastal and mid-gyre upwelling (Astraldi and Gasparini, 1995).

Surface salinity in the Tyrrhenian Sea is low because of the dominant influence of MAW advected by the Algerian Current. Typical MAW characteristics are clear seasonal changes and large horizontal gradients. Salinity values range from 36.8 for the newly incoming water, to 38.2–38.4 in the central parts of the northern and southern gyres, which are influenced by intensive mixing with saline subsurface water (Astraldi and Gasparini, 1995). Along with mid-gyre upwelling, temperature anomalies of 6°C (seasonal range of 13°–16°C in the central gyre opposed to 14°–22° outside the gyre; Marullo et al., 1995) are observed.

The hydrography at the Balearic Rise and in the Tyrrhenian Sea is thus strongly influenced by the advection of Atlantic waters and associated changes in temperature and salinity. Upwelling of intermediate waters that come from eastern Mediterranean sources additionally control surface water conditions. The range of hydrographic change that goes along with this variability must be kept in mind when interpreting estimates of paleotemperature and salinity at both sites.

METHODS

Alkenone Analyses

Following the method of Prahl et al. (1995), lipid extractions and compound class isolation for gas chromatography were used to analyze long-chain alkenones. Two to 5 g of freeze-dried sediment were extracted three times by ultrasonicating for 20 min using a 1:3 mixture of toluene and methanol. The extracts were combined in a separator funnel and acids were removed by extraction with 0.5 *N* KOH. The residual fraction was pre-dried with Na_2SO_4, and then evaporated with a rotary evaporator until dry. The dried fraction was then redissolved in 1 mL of hexane for column chromatography. Lipids were separated into compound classes by silica gel chromatography. Before separation, the silica gel (70–230 mesh, Merck) was activated by heating at 220°C for 24 h. After cooling, the silica gel was deactivated by 5%. With 7 g of silica gel a 11-cm column (1.5-cm inner diameter [i.d.]) was prepared and rinsed with the solvent of the first fraction (hexane). Re-dissolved lipids were loaded into the silica gel. Compound classes were separated by sequential solvent treatment: (1) 35 mL hexane (100%), (2) 40 mL toluene in hexane (25%), (3) 25 mL ethyl acetate in hexane (5%), (4) 15 mL ethyl acetate in hexane (10%), (5) 25 mL ethyl acetate in hexane (15%), and (6) 50 mL ethyl acetate in hexane (29%). Alkenones and alkenoates eluted in the third fraction.

Relative alkenone abundances were determined by flame ionization detection gas chromatography (GC/FID) using a Carlo Erba GC4130 Fractovap gas chromatograph with a split injection system. A 30-m-long J&W Scientific DB-1 fused silica capillary with a 0.25 µm film thickness and an i.d. of 0.25 mm was used for analysis. Oven temperature was programmed to heat from 140° to 300°C at a rate of 5°C/min and then maintained at 300°C for 30 minutes. Hydrogen was used as a carrier gas at a pressure of 0.8 kg/cm^2. An alkenone-containing mud standard with known alkenone concentrations as previously determined by GC–mass spectrometry was provided by F. Prahl and was routinely run for identification of alkenone compounds in the chromatograms. Extraction efficiency was checked by using an internal standard with known C_{19}-10-one concentration, a further nC_{36} standard was used to check for GC conditions. The unsaturation index $U^{k'}_{37}$ was calculated as $U^{k'}_{37} = [C_{37:2} / (C_{37:2}+C_{37:3})]$. SST was estimated from the $U^{k'}_{37}$ values using the alkenone paleotemperature equation of Prahl and Wakeham (1987),

$$U^{k'}_{37} = 0.034 \times T + 0.039, \quad (1)$$

which was established from laboratory cultures of *E. huxleyi* the primary alkenone producer in the modern ocean (Volkman et al., 1980). $U^{k'}_{37}$ indices have been calculated down to alkenone concentrations of 2 ng/g of dry sediment, but the signal-to-noise ratio started to increase significantly at concentrations below 10 ng/g of dry sediment, and we consider these $U^{k'}_{37}$ indices less reliable. TOC concentrations outside the TOC maxima that signify the (relict) sapropels are below 0.2 wt% and alkenone concentrations on occasion were too low to yield reliable $U^{k'}_{37}$ indices. Using alkenone measurements was thus not useful to obtain reliable SST estimates for "normal" hydrographic conditions before and after sapropel formation.

Stable Isotope Measurements

Stable isotope measurements were done in the isotope laboratory of the Geological Institute in Zurich using samples both from within sapropel horizons and from the sediments immediately adjacent to the sapropels. The measurements were made on planktonic foraminifer *G. bulloides* from the size fraction >250 µm. On average, 20 specimens were used per measurement. Prior to isotope analysis, the foraminifer shells were rinsed with distilled water, carefully crushed to release potential sediment fillings, re-washed, and then transferred to the carbonate preparation device. There, the samples were put in an automated ISOCARB system to react with 100% phosphoric acid in a vacuum at 90°C to release the sample CO_2. The CO_2 was transferred online to a VG-Prism mass-spectrometer for isotope analysis. The NBS18, NBS19, and NBS20 carbonate standards were used to calibrate the mass spectrometer to the international PDB scale. Long-term reproducibility of the measurements was better than 0.1‰ as determined from replicate measurements of internal laboratory standards. The isotope values are reported on the conventional PDB scale.

Organic Carbon Measurements

Shipboard total organic carbon concentration (TOC) and carbonate measurements were used here to recognize sapropel horizons at Sites 974 and 975. Shipboard analytical techniques and data lists are given in Comas, Zahn, Klaus, et al. (1996). These data were complemented by additional TOC measurements that were made at GEOMAR using a LECO Carbon Analyzer. The carbonate and TOC data are listed in Table 1 on CD-ROM (back pocket, this volume).

Reconstruction of Sea-Surface Paleohydrography

Oxygen isotope paleotemperature equations are a viable tool to reconstruct sea-surface paleotemperature or paleosalinity from planktonic foraminiferal $\delta^{18}O$. Here we use the paleotemperature equation of Erez and Luz (1983),

$$T = 17.0 - 4.52\,(\delta_c - \delta_w) + 0.003\,(\delta_c - \delta_w)^2, \quad (2)$$

which was calibrated from laboratory cultures of planktonic foraminifers at a range of water temperature from 14° to 30°C. In Equation 2, δ_c and δ_w are the $\delta^{18}O$ values of foraminiferal calcite and ambient seawater, respectively. Using the SST estimates derived from the alkenone measurements and our planktonic $\delta^{18}O$ data as values for T and δ_c, Equation 1 can be solved for δ_w. Throughout the world ocean, δ_w is linearly related to salinity through evaporation, which enriches salt and ^{18}O in surface waters (Craig and Gordon, 1965). For the Mediterranean, the relation between seawater δ_w and salinity has been recently re-evaluated by Pierre (in press) to be

$$\delta_w = 0.27 \times S - 8.9\ (r^2 = 0.87), \quad (3)$$

where S is salinity and –8.9 represents the regional freshwater δ_w in ‰ SMOW (Fig. 1; Pierre, in press). Equation 3 is different from the δ_w-S relation of Stahl and Rinow (1973), which uses a slope of 0.43 and a freshwater δ_w value of –14.85‰ SMOW for the Mediterranean. The offsets in slope and freshwater δ_w between the equations likely reflect the more detailed coverage by Pierre (in press), who made over 300 measurements across the entire Mediterranean.

Before using the foraminiferal isotope values as δ_c in Equation 3, we need to correct the values for $\delta^{18}O$-disequilibrium effects of *G. bulloides* and for long-term variations in mean-ocean δ_w that were associated with glacial-interglacial ice volume changes. Comparing $\delta^{18}O$ values of core top samples from the northern North Atlantic with ambient surface-water temperature and δ_w has shown that the

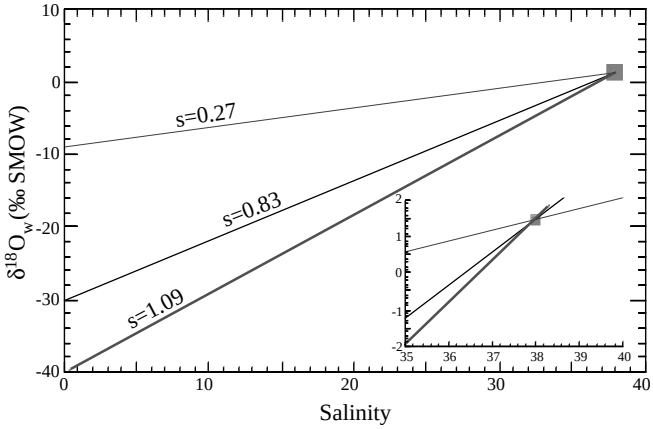

Figure 1. Seawater $\delta^{18}O$ (δ_w)-salinity relationships using different end-member δ_w and slopes. Modern relation values of –8.9‰ SMOW and s = 0.27 are from Pierre (in press). Depleted δ_w values of –30‰ and –40‰ SMOW and steeper slopes are used for sensitivity tests. Solid square shows modern mean Mediterranean salinity.

temperature deduced from *G. bulloides* $\delta^{18}O$ differs from the observed summer SST by as much as –1°C (Duplessy et al., 1991). The comparison also revealed that $\delta^{18}O$ of *G. bulloides* is closely correlated to SST (at the constant offset of –1°C) only within the range of 7°–22°C (Duplessy et al., 1991). Even though paleotemperatures as derived from $U^{k'}_{37}$ indices are occasionally warmer than 22°C, we correct the *G. bulloides* $\delta^{18}O$ values at Sites 974 and 975 for apparent $\delta^{18}O$ disequilibrium effects by subtracting 0.25‰ to account for the temperature offset of –1°C.

For mean-ocean δ_w "ice-effect" corrections, we used the δ_w record of Vogelsang (1990), which spans the past 400 k.y. and displays a mean glacial-interglacial δ_w amplitude of 1.1‰. This is in agreement with similar estimates from coral growth functions (Fairbanks, 1989). After δ_w has been calculated from Equation 2, salinity can be estimated by using δ_w as input into Equation 3. An apparent weakness of this strategy is that Equation 3 represents modern δ_w-S conditions in the Mediterranean and may not adequately represent hydrographic conditions during glacial periods and during times of sapropel formation. Enhanced freshwater input from melting alpine glaciers and from increased precipitation over the northern Mediterranean borderlands likely resulted in shifts of freshwater δ_w and the slope of the δ_w-S relation, as did variations of the regional evaporation-precipitation balance. We test the sensitivity of our salinity estimates to potential changes in freshwater δ_w by using hypothetical freshwater δ_w end-members of –30‰ SMOW and –40‰ SMOW, which steepen the slope of the δ_w-S relation to 0.8 and 1.1, respectively (Fig. 1). The sensitivity test is designed to demonstrate the change in estimated salinity as a function of the δ_w-S condition. Detailed reconstruction of salinity from foraminiferal $\delta^{18}O$ and SST estimates warrants independent information on the possible range of changes in δ_w, S, and E–P that may have occurred under an array of climatic boundary conditions during the past. This evaluation must come from an integration of terrestrial and marine paleodata in combination with numerical modeling of the hydrologic cycle and associated isotope effects.

Stratigraphic Correlation of Sapropels Between Sites 974 and 975

In our study we focus on selected sapropel intervals at Sites 974 and 975 (Murat, Chap. 41, this volume; Fig. 2). Correlation of the sapropel events between both sites was done using the $\delta^{18}O$ stratigraphy from Site 975 (Pierre et al., Chap. 38, this volume) and biostratigraphic age assignments for Site 974 (de Kaenel et al., Chap. 13, this

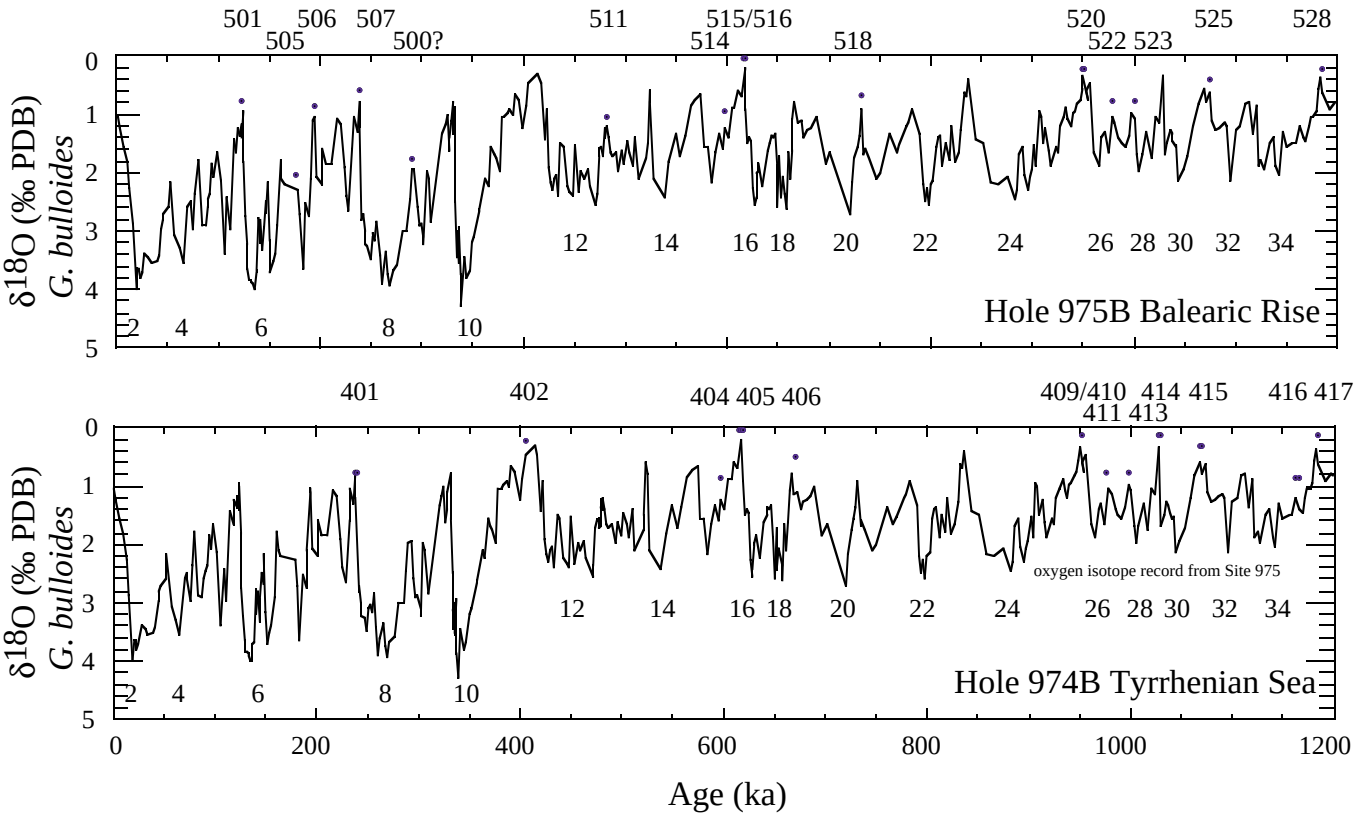

Figure 2. Stratigraphic overview of sapropels (solid dots) at Balearic Rise Site 975 and Tyrrhenian Sea Site 974. The oxygen isotope stratigraphy (solid line) for Site 975 is from Pierre et al. (Chap. 38, this volume). The isotope record is also plotted for Site 974 for which no isotope record has been established to date. The Site 974 time scale has been developed by de Kaenel et al. (Chap. 13, this volume).

volume; Fig. 2). From this stratigraphic framework it can be deduced that a number of sapropels that we analyzed for alkenone concentrations coevally exist at both sites (Fig. 2): 401–507, 404–514, 405–515/516, 411/412–522, 413–523, 415–525 (for sapropel indexing see Murat, Chap. 41, this volume). These sapropels can thus be used to estimate regional gradients between the Balearic Rise and the Tyrrhenian Sea. Using the detailed $\delta^{18}O$ stratigraphy of Pierre et al. (Chap. 38, this volume) for Site 975, it can be further deduced that the uppermost sapropel 501 at Site 975 most likely correlates with eastern Mediterranean type-sapropel S5 that has an orbital age of 124 ka (Lourens et al., 1996). Likewise, sapropels 505, 506, and 507 appear to correlate with eastern Mediterranean type-sapropels S6, S7, and S9, which have been orbitally dated by Lourens et al. (1996) to 172 ka, 195 ka, and 240 ka, respectively. The stratigraphic scheme for Site 975 also implies that there is no sapropel at the Balearic Rise that would be coeval with eastern Mediterranean sapropel S8. For detailed correlations of the western Mediterranean sapropels and organic-rich layers, see Murat (Chap. 41, this volume) and de Kaenel et al., Chap. 13 (this volume).

RESULTS

TOC and $CaCO_3$

TOC concentrations for sapropels vary between 0.89 and 4.48 wt% at Site 974 and between 0.60 and 2.65 wt% at Site 975 (Fig. 3). TOC concentrations in "normal" sediments above and below the sapropels are about 0.2 wt% at both sites. Enhancement of TOC concentrations at Site 974 over those observed at coeval sapropels at Site 975 may reflect higher productivity and/or higher preservation of organic carbon in the Tyrrhenian Sea.

$CaCO_3$ concentrations at Site 974 show some variation across sapropel intervals, but the changes are small. Distinct $CaCO_3$ minima are documented for sapropels 409/410, 415, and 416 (Fig. 3). A decrease in $CaCO_3$ concentration would be expected when, during sapropel formation, enhanced input of partially degraded organic material releases dissolved CO_2, which makes the pore waters corrosive to $CaCO_3$ (e.g., Emerson and Archer, 1990). Sapropels 405 and 406 are associated with $CaCO_3$ maxima even though TOC contents are high, around 2–3 wt% (Fig. 3). In general, $CaCO_3$ concentrations are higher at the Balearic Rise (Site 975) than in the Tyrrhenian Sea (Site 974).

Concentrations of Alkenones and $U^{k'}_{37}$ Indices

Alkenone concentrations ($C_{37:3}$ and $C_{37:3}$) in sapropels vary between 446 and 2056 ng/g of dry sediment at Site 974 and between 522 and 2297 ng/g of dry sediment at Site 975. Fluctuations in alkenone concentration directly correlate with changes in TOC concentration in that highest concentrations of $C_{37:3}$ and $C_{37:3}$ alkenones correlate with maximum TOC concentrations (Fig. 3). Alkenone concentrations are exceptionally low in sapropels 507, 508, and 518 at Site 975, between 10 and 24 ng/g of dry sediment. On average, alkenone concentrations are higher in the sapropels at Site 974, in agree-

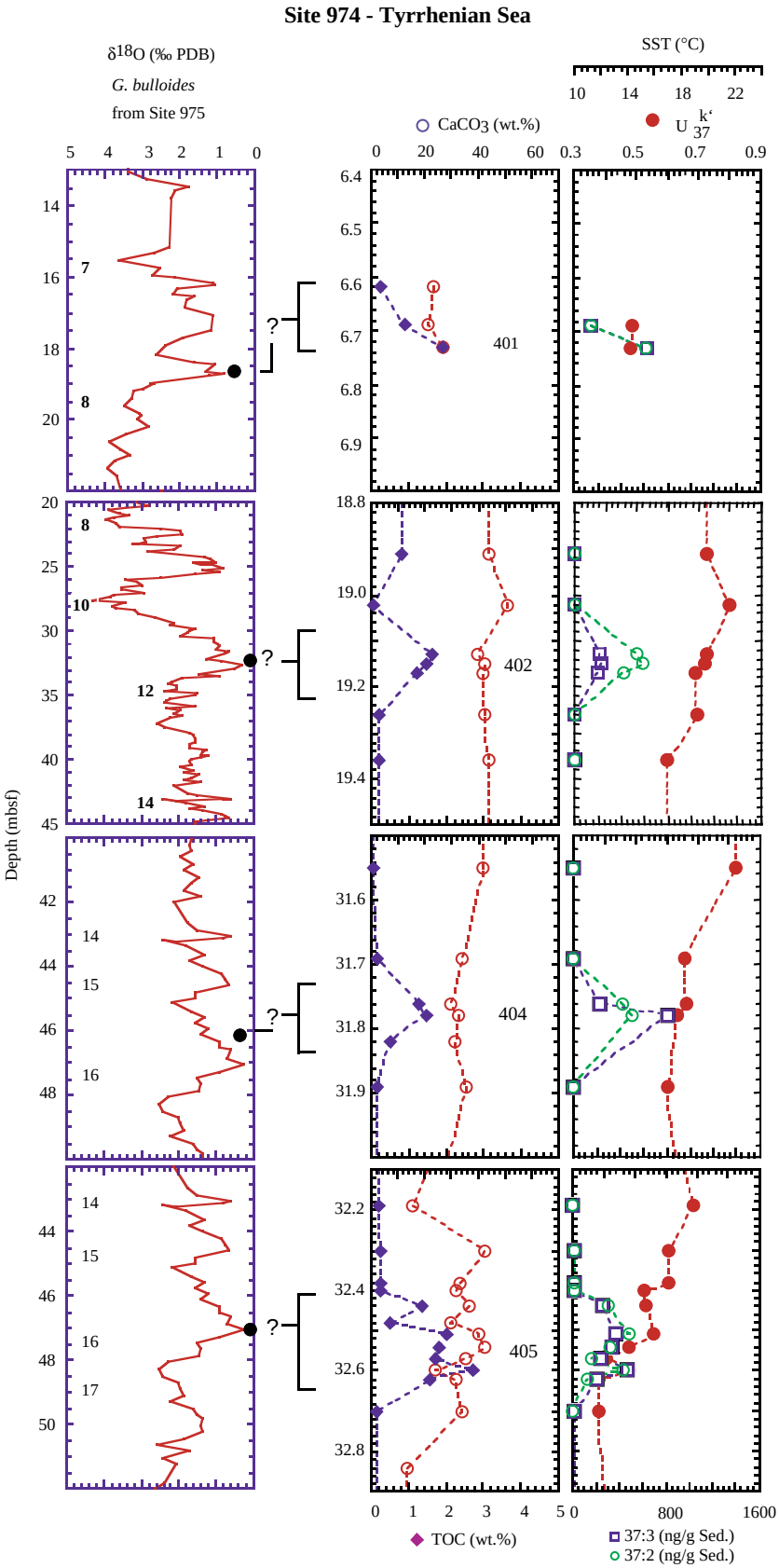

Figure 3. Results of TOC, $CaCO_3$, and alkenone concentrations of sampled sapropels from Hole 974B and 975B compared with results of the $U^{k'}_{37}$ index. (Continued next page.)

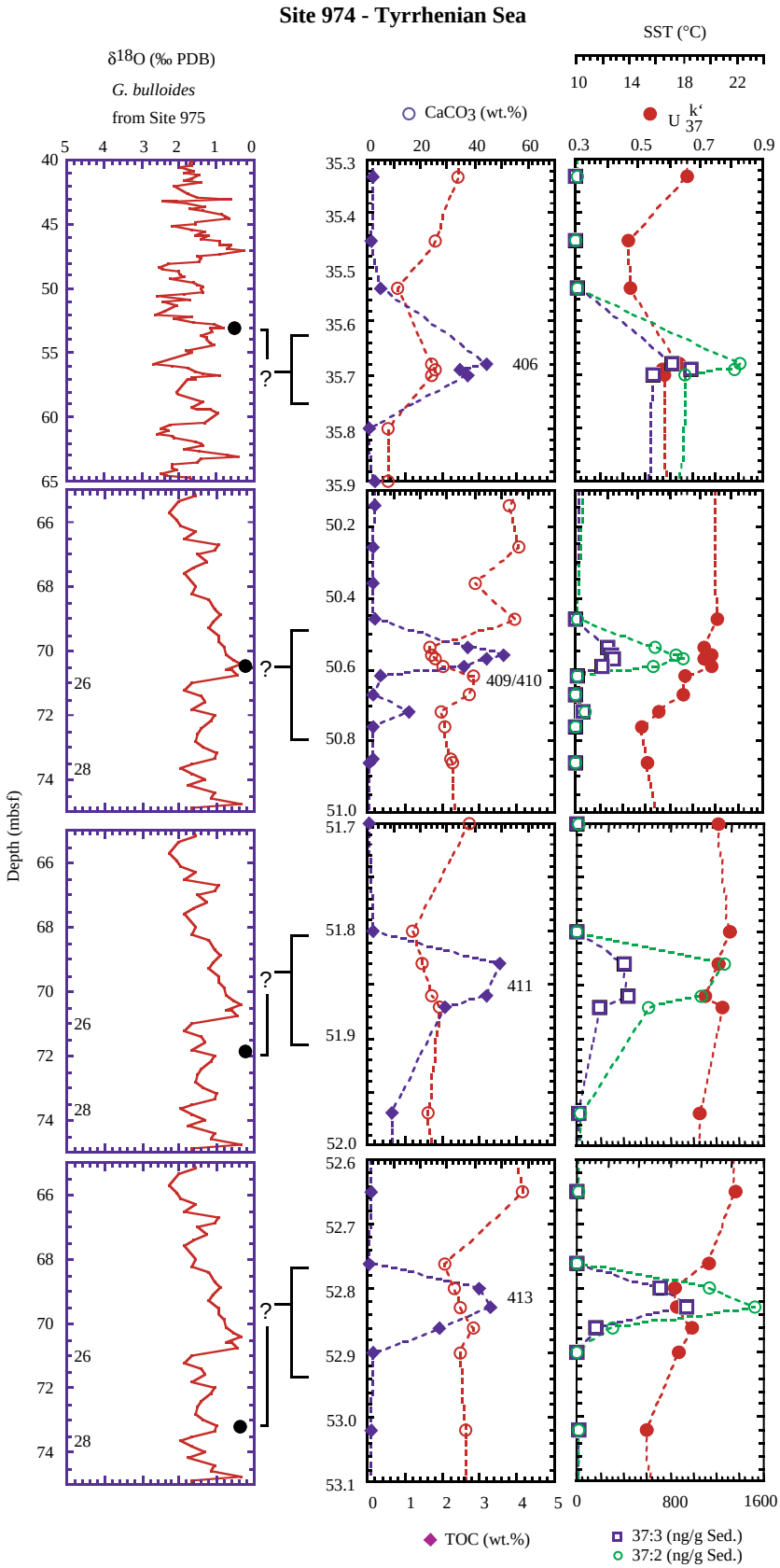

Figure 3 (continued).

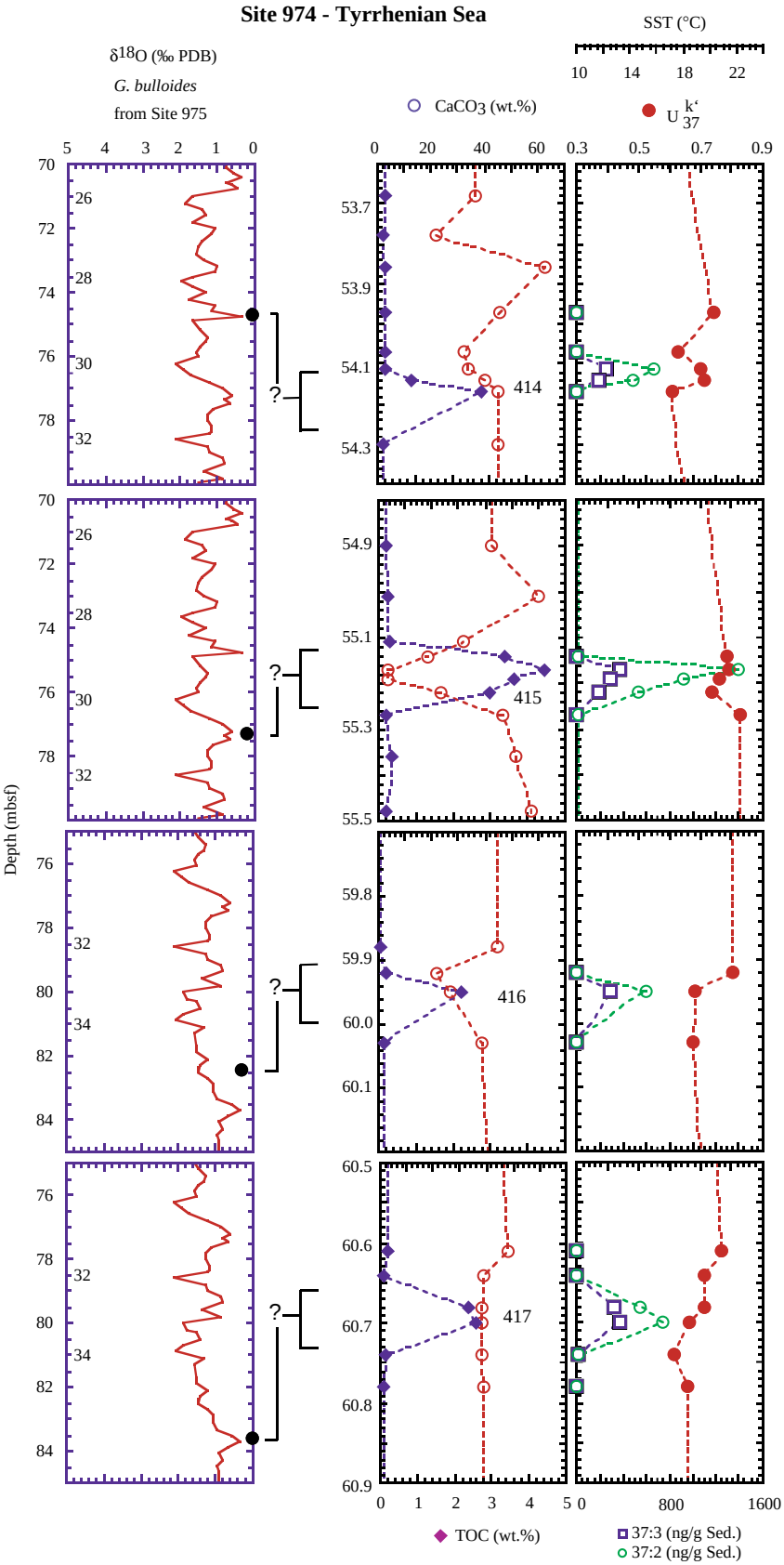

Figure 3 (continued).

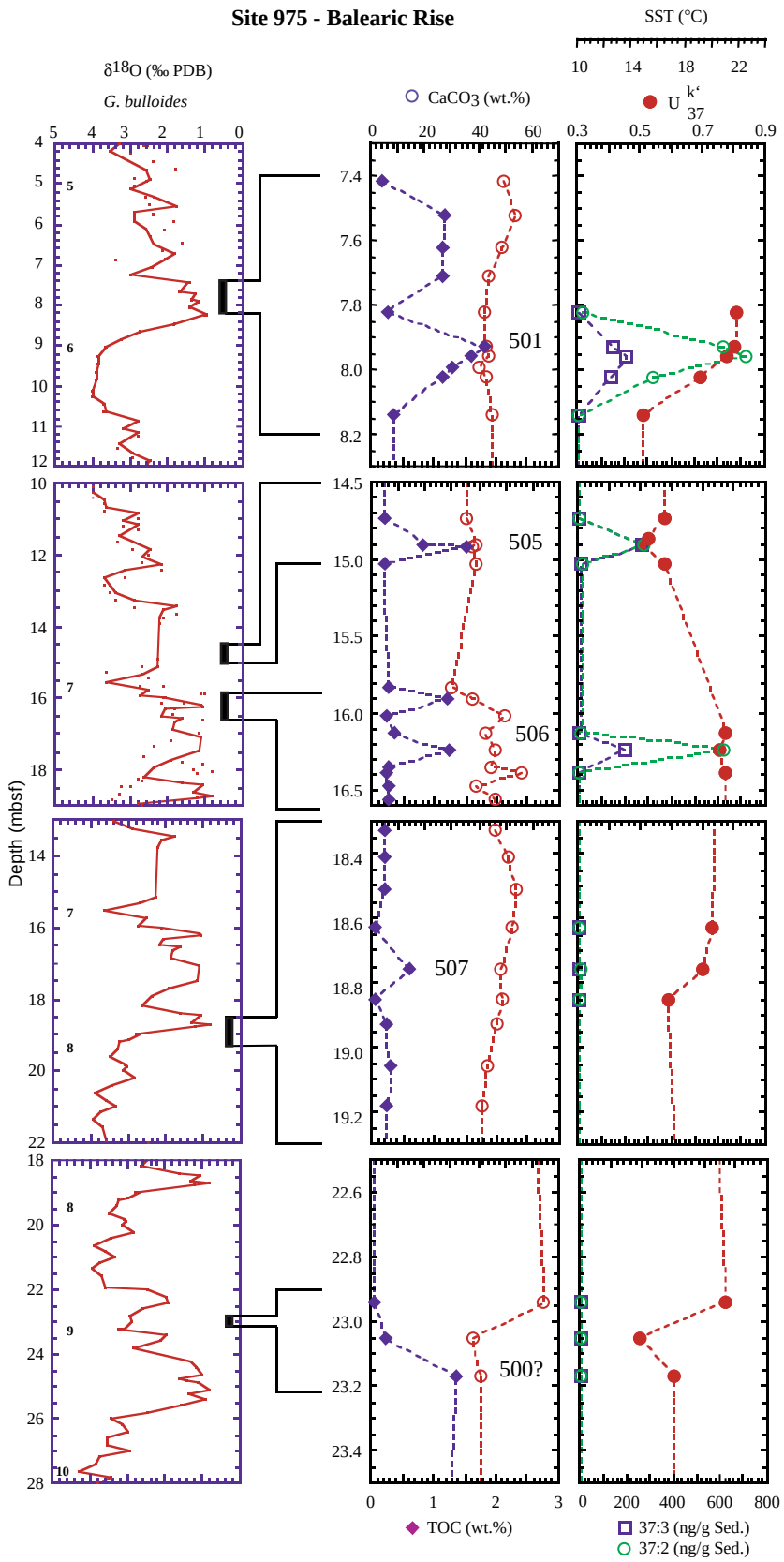

Figure 3 (continued).

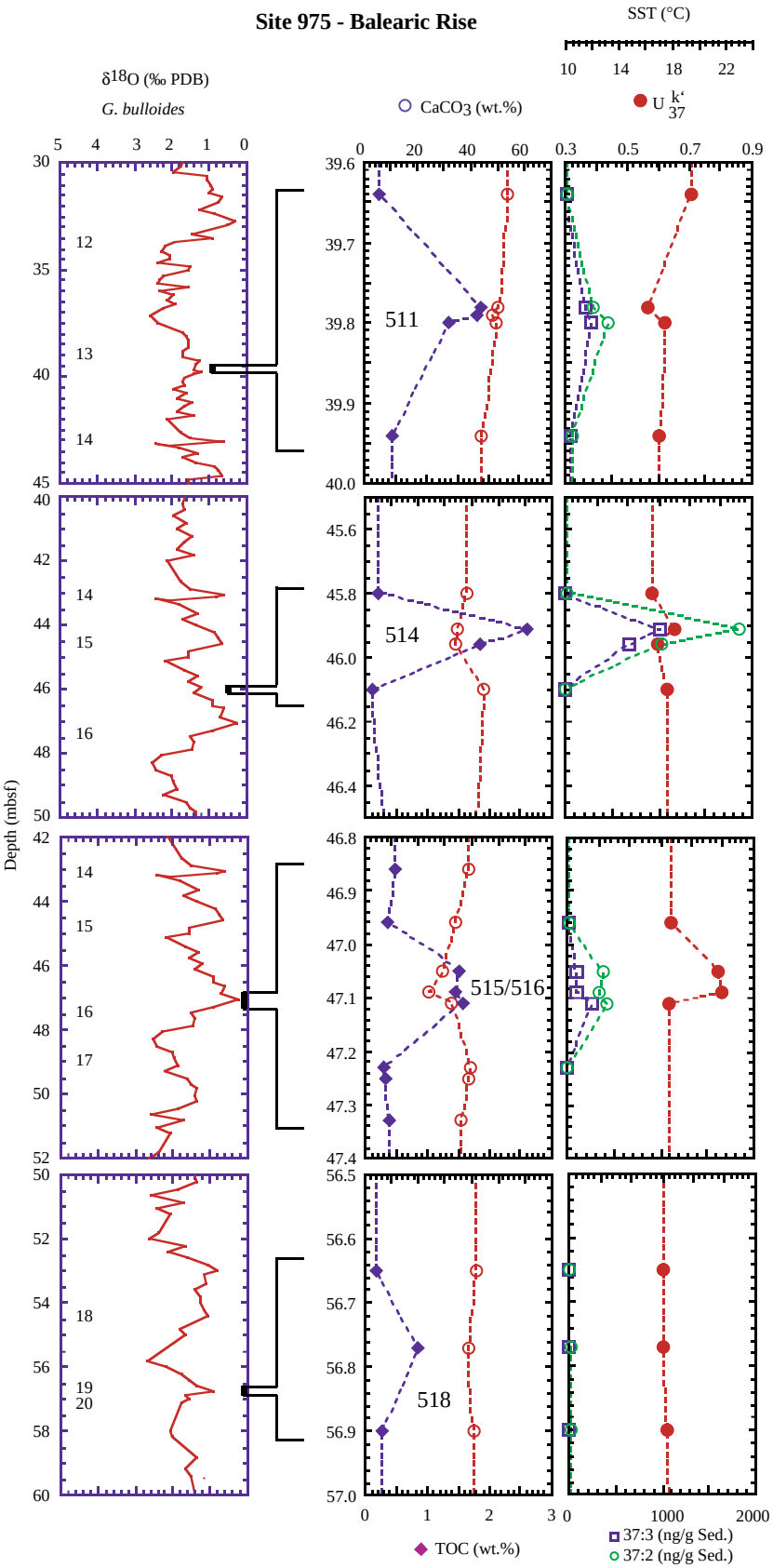

Figure 3 (continued).

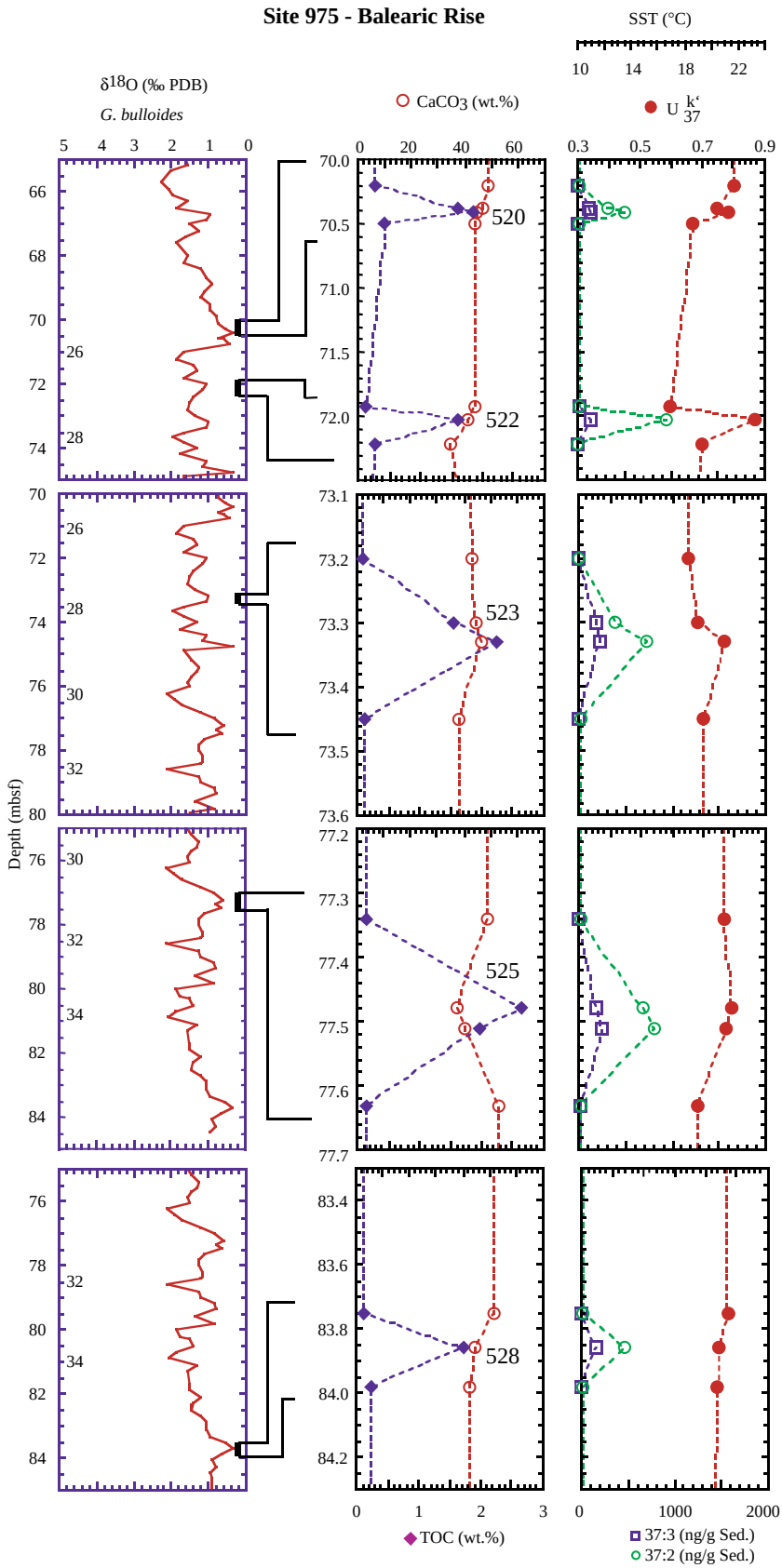

Figure 3 (continued).

ment with the higher TOC concentrations. The only exceptions are sapropels 404 (Site 974) and 514 (Site 975), which are coeval (Fig. 2). In this case, TOC and alkenone concentrations are higher at Site 975. Alkenone concentrations outside the horizons of enhanced TOC concentrations are below 10 ng/g of dry sediment, so the derived $U^{k'}_{37}$ indices are questionable in these cases.

The range of $U^{k'}_{37}$ values is 0.383–0.826 at Site 974 and 0.474–0.874 at Site 975. In most cases $U^{k'}_{37}$ values increase during TOC maxima, whereas, within individual sapropels, $U^{k'}_{37}$ changes are small (Fig. 3). For some cases, a trend of increasing $U^{k'}_{37}$ values towards the top of sapropels is observed (Site 974: 402, 404, 405, 415, 417; Site 975: 501; Fig. 3), possibly indicating that the upper boundary of the TOC maximum does not represent the upper boundary of the original sapropel but rather coincides with the position of the oxidation front that led to the burn-down of organic carbon (De Lange et al., 1989; Pruysers et al., 1993). An opposite trend of decreasing $U^{k'}_{37}$ values (occurring partially at $U^{k'}_{37}$ levels that are increased above background) is observed at Site 974 for sapropels 409/410, 413, and 414, and at Site 975 for sapropels 511, 515/516, 520, and 523.

DISCUSSION

SST Derived From $U^{k'}_{37}$ Indices

To estimate SST from the $U^{k'}_{37}$ indices we use the alkenone paleotemperature equation of Prahl and Wakeham (1987; Equation 1, above). This equation was calibrated using *E. huxleyi* from laboratory cultures. An alternate $U^{k'}_{37}$ paleotemperature equation was established by Ternois et al. (1997) from sediment trap samples that cover a temperature range of 13–19°C (equivalent to a $U^{k'}_{37}$ range of 0.3–0.55). The range of $U^{k'}_{37}$ values is 0.38–0.87, but the majority of values clusters around 0.6–0.7 (i.e., at higher levels than the range obtained by Ternois et al. [1997] for calibration of their equation). For this reason we chose Equation 1 to estimate the SST fluctuations shown in Figures 3 and 4. However, in the following sections we will discuss SST estimates derived from both equations and their implications for our salinity estimates.

The alkenone paleotemperature equations of Prahl and Wakeham (1987) and Ternois et al. (1997) were established from measurements on *E. huxleyi*, which first appears in the geologic record around 270 ka and reaches its first common occurrence at 218 ka (de Kaenel et al., Chap. 13, this volume, and discussion therein). Therefore, application of these equations is formally limited to the stratigraphic record back to early-to-mid oxygen isotope stage 8. This stratigraphic range covers sapropels 401 at Site 974 and 501–507 at Site 975 (Fig. 2). Volkman et al. (1995) demonstrated that $U^{k'}_{37}$ ratios of *Gephyrocapsa oceanica* are also temperature dependent. From the coherent pattern in alkenone production for *E. huxleyi* and *G. oceanica*, it seems that the trend of increasing $U^{k'}_{37}$ indices with increasing temperature generally holds true in phytoplankton alkenone production, independent from the actual alkenone-producing phytoplankton species. Thus, we expand the use of equation 1 to $U^{k'}_{37}$ indices that were derived from alkenone measurements on sapropels older than the first appearance of *E. huxleyi*. In these cases, however, the SST scales in

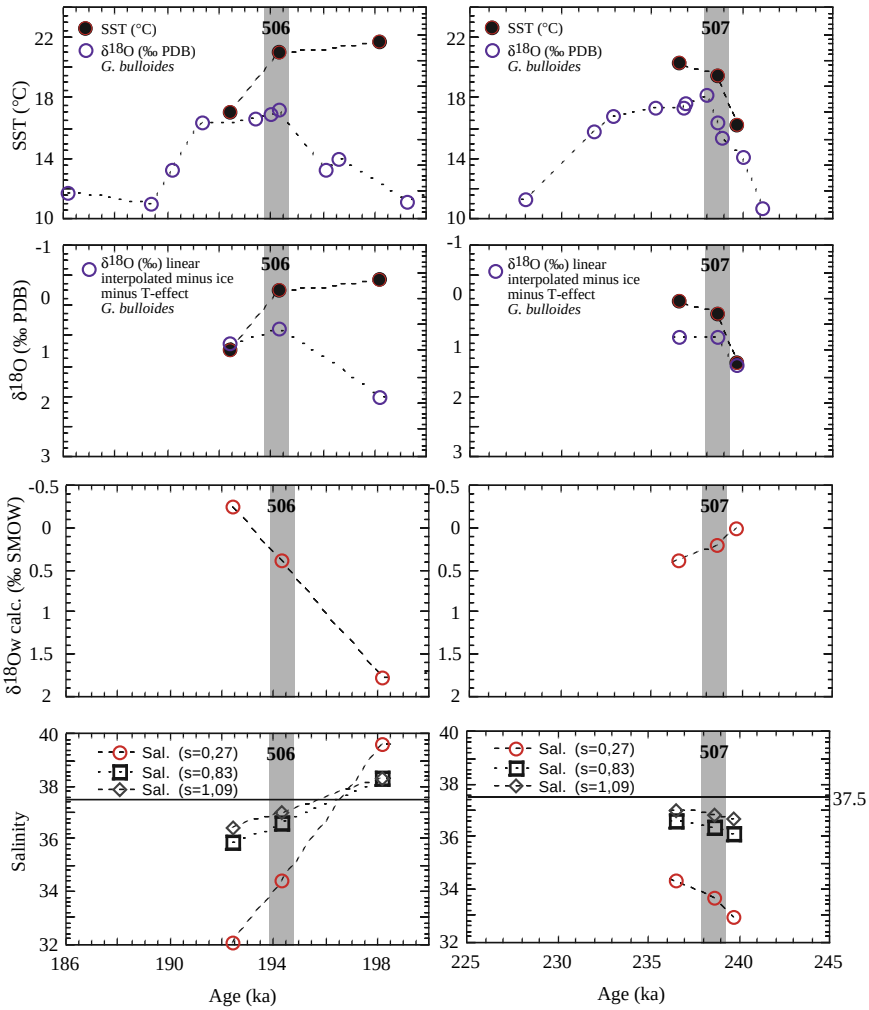

Figure 4. Reconstructions of salinity ranges during the formation of sapropels 506 and 507 at the Balearic Rise.

Figures 3 and 4 must be considered uncalibrated scales that approximate the magnitude of apparent SST changes.

SST estimates derived from $U^{k'}_{37}$ indices in sapropel samples at Site 974 and 975 are between 13° and 25°C (Table 2). Using the planktonic $\delta^{18}O$ record at Site 975 as a guide (Fig. 2), the sapropels cluster into "interglacial" sapropels that formed during fully interglacial periods (e.g., sapropels 501, 506, 507, 515 etc.; see Fig. 2) and into "glacial" sapropels that formed during glacial periods (sapropel 505). This grouping is also expressed in the SST pattern (Table 2) in that SST estimates for "interglacial" sapropels are on average 5°C warmer than those for "glacial" sapropels. This grouping is less obvious in the SSTs pattern for Site 974 sapropels. For this site there is no oxygen isotope stratigraphy available to date, so that the time scale was developed from biostratigraphic marker events alone (de Kaenel et al., Chap. 13, this volume). A detailed evaluation of the age scale and the position of the sapropels with respect to climatic stages and/or substages is not possible. Therefore, the irregular SST pattern between "interglacial" and "glacial" sapropels at Site 974 may in part be an artifact of stratigraphic weaknesses.

The cold SST estimates for sapropels 401 and 405, for instance, may be considered to be a clear indication that both sapropels did not develop during full interglacial stages 7.5 and 17, as inferred from the biostratigraphic age scale. Rather they may have formed during the latest glacial stages 8 and 18, or during the stage 7/8 and 17/18 climatic transitions. This contention is supported by similar evidence from Alboran Sea Sites 976 and 977, of which both have detailed oxygen isotope records. The records show that organic-rich layers there do not strictly correlate with $\delta^{18}O$ minima but occur both during fully glacial and fully interglacial conditions, as well as during climatic transitions (e.g., during the Younger Dryas rather than during the early Holocene climatic optimum [von Grafenstein et al., Chap. 37, this volume]). Despite this stratigraphic uncertainty, it appears that SST variability between individual sapropels is smaller at Site 974 than at Site 975.

The evolution of SST across sapropel horizons indicates that sapropel formation in most cases went along with warming (Fig. 3). This trend is best observed at Site 974 for sapropels 402, 404, 405, 411, and 417, and, at Site 975, for sapropels 501, 507, 514, and 525. In some cases warming appears to continue above the TOC maximum as inferred from increased $U^{k'}_{37}$ indices in samples from immediately above the horizon with enhanced TOC concentrations (Site 974: sapropels 402, 404, 405; Site 975: sapropels 507, 520, 528). Postdepositional oxidation of sapropels by downward moving oxygenation fronts (so-called burn-down; De Lange et al., 1989; Pruysers et al., 1993) has been shown to reduce thicknesses of TOC maxima. Degradation of organic matter by oxidation has been demonstrated to also affect the distribution pattern of higher ($C_{37:3}$) vs. lower unsaturated alkenones ($C_{37:2}$; e.g., Ficken and Farrimond, 1995; Flügge, 1997; see also discussion in Prahl et al., 1989). During oxidation, the $C_{37:3}$ alkenones are preferentially removed, leaving the remaining organic matter enriched in $C_{37:2}$ alkenones. The net effect of this process is an increase of the $U^{k'}_{37}$ index that simulates higher temperatures. This process appears to work most efficiently in cold water conditions (Flügge, 1997; Hoefs et al., 1998). The trend of increasing SST above some TOC maxima at Sites 974 and 975 may thus be the result of postdepositional TOC oxidation and associated alkenone degradation. There are, however, examples at Site 974 where alkenone concentrations decrease rapidly above TOC maxima (sapropels 401, 404, 414), but the $U^{k'}_{37}$ index and estimated SST remain nearly constant or even decrease. In view of this evidence, it still appears conceivable that increasing SST above some TOC maxima reflects true surface water warming during sapropel formation that lasted longer than implied by the thickness of the (relict) TOC maximum.

As shown in Table 2, SST estimates for sapropels at Sites 974 and 975 range between 13° and 25°C. These SSTs have been estimated by using the alkenone paleotemperature equation of Prahl and Wakeham (1987). Using the alkenone temperature calibration equation of Ternois et al. (1997), SST estimates for interglacial sapropels at Site 975 (sapropels 501, 506, 507) would be 2.5°C warmer on average whereas for glacial sapropel 505, an ~3.8°C warmer SST would be indicated. Mean annual SST today at the Balearic Rise is 19.5°C with a seasonal range of 15°C for winter to 24°C for summer (Levitus, 1982). Our SST estimates for interglacial sapropels at the Balearic Rise thus imply that temperatures were on average between 2° and 4.5°C warmer than mean annual SSTs today, making them close to modern summer SST. Our $U^{k'}_{37}$ SST estimates for glacial sapropels are well within or slightly warmer than the seasonal SST range of 9°C for winter and 16°C for summer that has been estimated for mean glacial conditions at the Balearic Rise from planktonic foraminifer census counts (Thiede, 1978). Mean annual SST today at Site 974 is 19.0°C with a seasonal range of 14° (winter) to 24°C (summer; Levitus, 1982). Mean glacial estimates for the central Tyrrhenian Sea range from 7°C in winter to 14°C in summer (Thiede, 1978). Lack of a $\delta^{18}O$ stratigraphy at this site inhibits detailed stratigraphic correlations but from our SST estimates (Table 2) it seems that coldest inferred SSTs are still well above the minimum mean glacial SST of 7°C and that SSTs significantly warmer than the modern mean annual SST of 19°C are recorded in only two cases (sapropels 411, 415; Table 2). But even the two warm examples with SSTs of 20.8°C and 21.5°C remain below modern summer SST. It thus appears that SST anomalies during sapropel formation at Site 974 were largest for "cold" sapropels and warm SST anomalies in the Tyrrhenian Sea were less distinct compared to Site 975 at the Balearic Rise.

Table 2. $U^{k'}_{37}$ indices and estimated sea-surface temperatures for sapropels at Sites 974 and 975.

Site 974 (Tyrrhenian Sea)			Site 975 (Balearic Rise)		
Sapropel*	$U^{k'}_{37}$	SST (°C)	Sapropel*	$U^{k'}_{37}$	SST (°C)
Interglacial					
401	0.490	13.3	501	0.769	21.5
402	0.710	19.7	506	0.757	21.1
405	0.474	12.8	507	0.702	19.5
406	0.599	16.5	515/516	0.736	20.5
409/410	0.652	18.0	520	0.767	21.4
411	0.746	20.8	522	0.874	24.6
413	0.635	17.5	523	0.724	20.2
414	0.716	19.9	525	0.781	21.8
415	0.770	21.5	528	0.741	20.6
417	0.645	17.8			
Glacial					
404	0.647	17.9	505	0.492	13.4
416	0.682	18.9	511	0.621	17.1
			514	0.626	17.3
			518	0.568	15.6

Note: *For sapropel indexing see Murat (Chap. 41, this volume).

$U^{k'}_{37}$-SST Estimates, Planktonic $\delta^{18}O$, and Provisional Salinity Estimates

A distinct feature of sapropel horizons is the occurrence of negative planktonic foraminiferal $\delta^{18}O$ excursions, which have been traditionally inferred to reflect surface water freshening caused by enhanced river runoff and precipitation in the course of orbitally driven insolation changes (Rossignol-Strick, 1985). Our SST estimates indicate, in agreement with recent concepts (e.g., Rohling, 1994), that sapropel formation went along with surface-water warming and, thus, that part of the negative $\delta^{18}O$ anomalies must come from temperature effects. To estimate potential changes in surface water hydrography, we follow the concept outlined above, that is, we use planktonic foraminiferal $\delta^{18}O$ and $U^{k'}_{37}$ paleotemperature estimates as values in an oxygen isotope paleotemperature equation, which we solve for δ_W to infer changes in surface water salinity (Table 3). Planktonic $\delta^{18}O$ has been corrected for global ice volume changes and disequilibrium effects (Vogelsang, 1990; Duplessy et al., 1991). We restrict our discussion to sapropels 506 and 507 at Site 975 be-

cause this site has a detailed $\delta^{18}O$ stratigraphy and both sapropels formed well after the first occurrence of *E. huxleyi,* which has been used to calibrate the $U^{k'}_{37}$ index to ambient SST. Both sapropels occur during fully interglacial stages 7.1 and 7.5 so that no correction has been applied for mean-ocean salinity changes.

In both cases, planktonic $\delta^{18}O$ displays well-developed negative anomalies (Fig. 4). The isotope anomalies start earlier and last longer than the TOC maxima, pointing both to early environmental change well before sapropel formation started and to post-depositional diagenetic burn-down of the upper parts of both sapropels. As in most other cases, TOC concentrations are too low in sediments above and below the TOC maximum to allow for detailed alkenone measurements. Thus, our SST estimates are confined to the immediate TOC maximum and do not reflect the evolution of SST from "normal" conditions sapropel formation into the sapropel and back to "normal" after sapropel formation had terminated. For sapropel 507, warming by 3°C from 17° to 20°C is indicated, which parallels the planktonic $\delta^{18}O$ depletion. For sapropel 506, on the other hand, inferred SST is high, around 22°C, in a single sample that was well below the TOC maximum. Within the TOC maximum, SST is slightly decreased (21°C), and then further decreased to around 17°C above the TOC maximum. This temperature evolution is in contrast to the planktonic $\delta^{18}O$ profile across sapropel 506, which shows a depletion that starts well before the TOC maximum and persists beyond the section where the $U^{k'}_{37}$ index already indicates surface water cooling (Fig. 4).

Estimated salinities for both TOC maxima at Site 975 are around 34, salinities above the TOC maxima are 32 for sapropel 506 and 34 for sapropel 507 (Table 3). Judging from the structure of the $\delta^{18}O$ anomaly, the salinity estimates from above the TOC maximum still represent sapropel conditions. This is true even though TOC is low, which is likely because of carbon burn-down. Surface salinity was decreased during the formation of both sapropels to between 32 and 34, which is considerably lower than the modern salinity of 37.5 at this location (Levitus, 1982). The salinity decrease is reduced by 2–4 units if the contribution of freshwater with more negative end-member δ_w of –30‰ and –40‰ SMOW (compared to –8.9‰ SMOW today) is assumed (Table 3). A possible source for strongly depleted δ_w is meltwater from alpine glaciers. But sapropels 506 and 507 formed during fully interglacial conditions, so that it appears unrealistic to infer meltwater as sources for extremely depleted δ_w, unless we assume that the deglacial meltwater supply lasted well into these fully interglacial periods. Still, using these extreme values for our calculation shows that the magnitude of inferred salinity changes greatly depends on the history of freshwater δ_w, which is dependent on the evolution of regional climates, especially the balance between evaporation and precipitation, and air temperature.

Comparison of estimated salinities from before and within sapropel 506 implies a salinity drop by 7 units. However, the pre-sapropel salinity of 39.6, ~3 k.y. before the sapropel formed, results from the combination of increased planktonic $\delta^{18}O$, which reflects cold oxygen isotope stadial 7.2 and warm SST estimates derived from our $U^{k'}_{37}$ data. In this sample, concentrations of $C_{37:3}$ alkenones are only 2 ng/g of dry sediment, and $C_{37:2}$ alkenones are only 7 ng/g of dry sediment. The warm SST estimate of nearly 22°C for substage 7.2 may thus be an artifact of low signal-to-noise ratio, possibly in combination with alkenone degradation during TOC oxidation. If so, salinities would have been higher than inferred by using the too-warm temperature estimate.

The evolution of surface salinity appears much different for sapropel 507 (Fig. 4; Table 3). Pre-sapropel salinities are estimated to be about 2 units lower than salinities during sapropel formation. The pre-sapropel sample was taken very close to the lower boundary of the TOC maximum and is within the late stage of the concurrent planktonic $\delta^{18}O$ depletion. Thus, depleted salinity inferred for this sample may not reflect true pre-sapropel conditions but rather the first freshwater incursions that led to sapropel formation shortly thereafter.

Table 3. Estimated seawater $\delta^{18}O$ (δ_w) and salinity for sapropels 506 and 507.

Sapropel	Age (ka)	δ_w (‰ SMOW)	Salinity* (s = 0.27)	Salinity† (s = 0.83)	Salinity** (s = 1.09)
506	192.4	-0.25	32.05	35.85	36.47
506	194.3	0.39	34.41	36.61	37.05
pre-506	198.2	1.79	39.59	38.3	38.34
507	236.5	0.37	34.34	36.59	37.04
507	238.6	0.20	33.70	36.38	36.88
pre-507	239.7	0.00	32.95	36.14	36.70

Note: * = freshwater δ_w = –8.9‰ SMOW; † = freshwater δ_w = –30‰ SMOW; ** = freshwater δ_w = –40‰ SMOW.

Even though we cannot detail the evolution of surface-water temperature and salinity in the course of sapropel formation, the two cases described above show that hydrographic patterns can be estimated if reliable SST estimates are available and if assumptions are made about hydrologic parameters such as freshwater end-member δ_w and the evolution of the δ_w-salinity relationship. From our study, it is also apparent that the $U^{k'}_{37}$ index is of limited help in SST estimation for the western Mediterranean, because, except for TOC-enriched sapropels and organic-rich layers, alkenone concentrations are too low for reliable SST reconstructions. These SST reconstructions must come from other sources such as evaluating temperature-sensitive dynocyst assemblages and planktonic foraminifer census counts (Combourieu Nebout et al., Chap. 36, this volume; Linares et al., Chap. 35, this volume; Serrano et al., Chap. 14, this volume).

SUMMARY AND CONCLUSIONS

Measurements of alkenone concentrations have been used to determine $U^{k'}_{37}$ indices for a suite of sapropels at Sites 974 and 975. Applying the $U^{k'}_{37}$ paleotemperature equation of Prahl and Wakeham (1987) implies that SSTs estimated for individual sapropels vary between 13°C and 25°C. "Interglacial" sapropels at Site 975 (formed during fully interglacial periods) display 5°C warmer SSTs on average than "glacial" sapropels (formed during glacial periods). SST estimates for the interglacial sapropels at Site 975 are all above mean annual modern SST of 19.5°C and are close to modern summer SST. SST estimates for glacial sapropels at this site are all within the estimated range of mean glacial SST (Thiede, 1978), and mostly group around glacial summer SSTs. Sapropels at Site 974 also group into "warm" and "cold" sapropels, but, in the absence of a $\delta^{18}O$ stratigraphy, we cannot determine with confidence climatic (glacial) vs. interglacial conditions for these sapropels. Coldest inferred SSTs at this site are still above minimum mean glacial SST of 7°C. SST estimates at Sites 974 and 975 thus support the hypothesis that sapropel formation was synchronous with warm climate anomalies (Rohling, 1994).

We have used planktonic foraminiferal (*G. bulloides*) $\delta^{18}O$ in conjunction with the $U^{k'}_{37}$-derived SST estimates to infer potential surface salinities during sapropel formation. $\delta^{18}O$ exhibits distinct negative anomalies during sapropel events. Our SST estimates indicate that part of the negative $\delta^{18}O$ anomaly is caused by surface water warming. After correcting the values for global ice volume changes and oxygen isotope disequilibrium effects, we use planktonic $\delta^{18}O$ and SST as values in an oxygen isotope paleotemperature equation and solve for δ_w (seawater $\delta^{18}O$). Applying the revised Mediterranean δ_w-salinity equation (Pierre, in press), we infer paleosalinities for two sapropels at Site 975 that formed after the first occurrence of *E. huxleyi,* which is the primary alkenone producer in the modern ocean and has been used previously to calibrate the alkenone paleotemperature equation. Paleosalinity estimates are between 32 and 34 for both sapropels, which is considerably lower than modern salinity of 37.5 at this location. The salinity offset is reduced by 2–4 units if freshwater end-members with more negative δ_w signatures are assumed. De-

tailed estimates of hydrographic conditions are not possible, but our data provide clear confirmation that sapropel formation in the western Mediterranean was synchronous with warm and moist climates.

ACKNOWLEDGMENTS

We thank D. Schulz-Bull at the Marine Sciences Institute at Kiel University for providing laboratory space and time to run our alkenone measurements. M. Yamamoto and R. Stax provided helpful reviews of the manuscript. Walter Hale and his staff at the Bremen Core Repository help us with our postcruise sampling. The Bremen Core Repository is jointly funded by the Ocean Drilling Program, the University of Bremen, and the Deutsche Forschungsgemeinschaft. This work was supported by the Deutsche Forschungsgemeinschaft under grant Za 157/10.

REFERENCES

Arnone, R.A., and La Violette, P., 1986. Satellite definition of the biooptical and thermal variations of coastal eddies associated with the African coast. *J. Geophys. Res.*, 91:2351–2364.

Artale, M., Astraldi, M., Buffoni, G., and Gasparini, G.P., 1994. Seasonal variability of gyre-scale circulation in the northern Tyrrhenian Sea. *J. Geophys. Res.*, 99, C7: 14,127–14,137.

Astraldi, M., and Gasparini, G.P., 1995. The seasonal characteristics of the circulation in the Tyrrhenian Sea. *In* La Violette, P.E. (Ed.), *Seasonal and interannual variability of the Western Mediterranean Sea.* Am. Geophys. Union, Coastal and estuarine studies, 46:115–134.

Béthoux, J.-P., 1993. Mediterranean sapropel formation, dynamic and climatic viewpoints. *Oceanol. Acta*, 16:127–133.

Cita, M.B., Vergnaud-Grazzini, C., Robert, C., Chamley, H., Ciaranfi, N., and D'Onofrio, S., 1977. Paleoclimatic record of a long deep sea core from the eastern Mediterranean. *Quat. Res.*, 8:205–235.

Comas, M.C., Zahn, R., Klaus, A., et al., 1996. *Proc. ODP, Init. Repts.*, 161: College Station, TX (Ocean Drilling Program).

Craig, H., and Gordon, L.I., 1965. Deuterium and oxygen-18 variations in the ocean and the marine atmosphere. *In* Tongiorgi, E. (Ed.), *Stable Isotopes in Oceanographic Studies and Paleotemperatures:* Pisa (Cons. Naz. delle Ric., Lab. di Geol. Nucleare), 9–130.

De Lange, G.J., Middelburg, J.J., and Pruysers, P.A., 1989. Discussion: Middle and Late Quaternary depositional sequences and cycles in the Eastern Mediterranean. *Sedimentology*, 36:151–158.

Deschamps, P.-Y., Frouin, R., and Crépon, M., 1984. Sea surface temperatures of the coastal zones of France observed by the HCMM satellite. *J. Geophys. Res.*, 89:8123–8149.

Duplessy, J.-C., Labeyrie, L., Juillet-Leclerc, A., Maitre, F., Duprat, J., and Sarnthein, M., 1991. Surface salinity reconstruction of the North Atlantic Ocean during the last glacial maximum. *Oceanol. Acta*, 14:311–324.

Emeis, K.-C., Doose, H., and Cacho-Lascorz, I., 1996. *Reconstruction of paleotemperatures during sapropel deposition based on high-resolution analyses of geochemical biomarkers in sediments.* Unpubl. Rep. EU-MAST, MAS2-CT93-0051.

Emeis, K.C., Schulz, H.-M., Struck, U., Sakamoto, T., Doose, H., Erlenkeuser, H., Howell, M., Kroon, D., and Paterne, M., 1998. Stable isotope and alkenone temperature records of sapropels from Sites 964 and 967: constraining the physical environment of sapropel formation in the Eastern Mediterranean Sea. *In* Robertson, A.H.F., Emeis, K.-C., Richter, C., and Camerlenghi, A. (Eds.), *Proc. ODP, Sci. Results*, 160: College Station, TX (Ocean Drilling Program), 309-331.

Emerson, S., and Archer, D., 1990. Calcium carbonate preservation in the ocean. *Philos. Trans. R. Soc. London A*, 331:29–40.

Emiliani, C., 1966. Paleotemperature analysis of Caribbean cores P-6304-8 and P-6304-9 and a generalized temperature curve for the past 425,000 years. *J. Geol.*, 74:109–124.

Epstein, S., Buchsbaum, R., Lowenstam, H.A., and Urey, H.C., 1953. Revised carbonate-water isotopic scale. *Geol. Soc. Am. Bull.*, 64:1315–1325.

Erez, J., and Luz, B., 1983. Experimental paleotemperature equation for planktonic foraminifera. *Geochim. Cosmochim. Acta*, 47:1025–1031.

Fairbanks, R.G., 1989. A 17,000-year glacio-eustatic sea level record: influence of glacial melting rates on the Younger Dryas event and deep-ocean circulation. *Nature*, 342:637–642.

Ficken, K.J., and Farrimond, P., 1995. Sedimentary lipid geochemistry of Framvaren: impacts of a changing environment. *Mar. Chem.*, 51:31–43.

Flügge, A., 1997. Jahreszeitliche Variabilität von ungesättigten C_{37} Methylketonen (Alkenonen) in Sinkstoffallenmaterial der Norwegischen See und deren Abbildung in Oberflächensedimenten [Ph.D. thesis]. Christian-Albrechts-Univ. Kiel.

Fontugne, M.R., and Calvert, S.E., 1992. Late Pleistocene variability of the carbon isotopic composition of organic matter in the eastern Mediterranean: monitor of changes in carbon sources and atmospheric CO_2 levels. *Paleoceanography*, 7:1–20.

Hemleben, C., and Spindler, M., 1983. Recent advances in research on living planktonic Foraminifera. *In* Meulenkamp, J.E. (Ed.), *Reconstruction of Marine Paleoenvironments. Utrecht Micropaleontol. Bull.*, 30:141–170.

Hilgen, F.J., 1991. Astronomical calibration of Gauss to Matuyama sapropels in the Mediterranean and implication for the geomagnetic polarity time scale. *Earth Planet. Sci. Lett.*, 104:226–244.

Hoefs, M.J.L., Versteegh, G.J.M., Rijpstra, I.C., de Leeuw, J.W., and Sinninghe Damsté, J.S., 1998. Postdepositional oxic degradation of alkenones: implications for the measurement of paleo sea surface temperatures. *Paleoceanography*, 13:42–49.

Hut, G., 1987. Stable isotope reference samples for geochemical and hydrological investigations. *Rept. to the Director General, Inter. Atomic Energy Agency, Vienna, 16–18 Sept. 1985.*

Imbrie, J., Hays, J.D., Martinson, D.G., McIntyre, A., Mix, A.C., Morley, J.J., Pisias, N.G., Prell, W.L., and Shackleton, N.J., 1984. The orbital theory of Pleistocene climate: support from a revised chronology of the marine $\delta^{18}O$ record. *In* Berger, A., Imbrie, J., Hays, J., Kukla, G., and Saltzman, B. (Eds.), *Milankovitch and Climate (Pt. 1), NATO ASI Ser. C, Math Phys. Sci.*, 126:269–305.

Kallel, N., Paterne, M., Duplessy, J.C., Vergnaud-Grazzini, C., Pujol, C., Labeyrie, L., Arnold, M., Fontugne, M., and Pierre, C., 1997. Enhanced rainfall in the mediterranean region during the last sapropel event. *Oceanol. Acta*, 20:697–712.

Kappertsbusch, M., 1993. Geographic distribution of living and Holocene coccolithophorides in the Mediterranean Sea. *Mar. Micropaleontol.*, 21:219–247.

Kidd, R.B., Cita, M.B., and Ryan, W.B.F., 1978. Stratigraphy of eastern Mediterranean sapropel sequences recovered during DSDP Leg 42A and their paleoenvironmental significance. *In* Hsü, K.J., Montadert, L., et al., *Init. Repts. DSDP*, 42 (Pt. 1): Washington (U.S. Govt. Printing Office), 421–443.

Kullenberg, B., 1952. On the salinity of the water contained in marine sediments. *Goeteborgs K. Vetensk. Vitterhets-Samh. Handl., Ser. B*, 6:3–37.

Levitus, S., 1982. Climatological Atlas of the World Ocean. *NOAA Prof. Pap.*, 13.

Lourens, L.J., Antonarakou, A., Hilgen, F.J., Van Hoof, A.A.M., Vergnaud-Grazzini, C., and Zachariasse, W.J., 1996. Evaluation of the Plio-Pleistocene astronomical timescale. *Paleoceanography*, 11:391–413.

Marlowe, I.T., Brassell, S.C., Eglinton, G., and Green, J.C., 1990. Long-chain alkenones and alkyl alkenoates and the fossil coccolith record of marine sediments. *Chem. Geol.*, 88:349–375.

Marlowe, I.T., Green, J.C., Neal, A.C., Brassell, S.C., Eglinton, G., and Course, P.A., 1984. Long chain (n-C_{37}-C_{39}) alkenones in the Prymnesiophyceae: distribution of alkenones and other lipids and their taxonomic significance. *Br. Phycol. J.*, 19:203–216.

Marullo, S., Santoleri, R., and Bignami, F., 1995. The surface characteristics of the Tyrrhenian Sea: historical satellite data analysis. *In* La Violette, P. (Ed.), *Seasonal and Interannual Variability of the Western Mediterranean Sea.* Am. Geophys. Union, Coastal and Estuarine Studies, 46:135–154.

Millot, C., 1987. Circulation in the western Mediterranean Sea. *Oceanol. Acta*, 10:143–149.

Nesteroff, W.D., 1973. Petrography and mineralogy of sapropels. *In* Ryan, W.B.F., Hsü, K.J., et al., *Init. Repts. DSDP*, 13: Washington (U.S. Govt. Printing Office), 713–720.

Olausson, E., 1961. Studies of deep-sea cores. *Rep. Swed. Deep-Sea Exped.*, 1947–1948, 8:335–391.

Pierre, C., in press.The oxygen and carbon isotope distribution in the Mediterranean water masses. *Mar. Geol.*

Prahl, F.G., De Lange, G.J., Lyle, M., and Sparrow, M.A., 1989. Post-depositional stability of long-chain alkenones under contrasting redox conditions. *Nature*, 341:434–437.

Prahl, F.G., Muehlhausen, L.A., and Zahnle, D.L., 1988. Further evaluation of long-chain alkenones as indicators of paleoceanographic conditions. *Geochim. Cosmochim. Acta*, 52:2303–2310.

Prahl, F.G., Pisias, N., Sparrow, M.A., and Sabin, A., 1995. Assessment of sea-surface temperature at 42° N in the California Current over the last 30,000 years. *Paleoceanography*, 10:763–773.

Prahl, F.G., and Wakeham, S.G., 1987. Calibration of unsaturation patterns in long-chain ketone compositions for paleotemperature assessment. *Nature*, 330:367–369.

Pruysers, P.A., De Lange, G.J., Middelburg, J.J., and Hydes, D.J., 1993. The diagenetic formation of metal-rich layers in sapropel-containing sediments in the eastern Mediterranean. *Geochim. Cosmochim. Acta*, 57:527–536.

Rohling, E.J., 1994. Review and new aspects concerning the formation of eastern Mediterranean sapropels. *Mar. Geol.*, 122:1–28.

Rossignol-Strick, M., 1985. Mediterranean Quaternary sapropels, an immediate response of the African Monsoon to variation of insolation. *Palaeogeogr., Palaeoclimatol., Palaeoecol.*, 49:237–263.

Rossignol-Strick, M., Nesteroff, W., Olive, P., and Vergnaud-Grazzini, C., 1982. After the deluge: Mediterranean stagnation and sapropel formation. *Nature*, 295:105–110.

Rostek, F., Ruhland, G., Bassinot, F.C., Muller, P.J., Labeyrie, L.D., Lancelot, Y., and Bard, E., 1993. Reconstructing sea surface temperature using $\delta^{18}O$ and alkenone records. *Nature*, 364:319–321.

Shackleton, N.J., 1969. The last interglacial in the marine and terrestrial record. *Proc. R. Soc. London*, 174:135–154.

Sonzogni, C., Bard, E., Rostek, F., Dollfus, D., Rosell-Mele, A., and Eglinton, G., 1997. Temperature and salinity effects on alkenone ratios measured in surface sediments from the Indian Ocean. *Quat. Res.*, 47:344–355.

Stahl, W., and Rinow, U., 1973. Sauerstoffisotopenanalysen an Mittelmeerwässern. Ein Beitrag zur Problematik von Paläotemperaturbestimmungen. *Meteor Forschungsergeb., Reihe C*, 14:5559.

Ternois, Y., Sicre, M.A., Boireau, A., Conte, M.H., and Eglinton, G., 1997. Evaluation of long-chain alkenones as paleo-temperature indicators in the Mediterranean Sea. *Deep-Sea Res.*, 44:271–286.

Thiede, J., 1978. A glacial Mediterranean. *Nature*, 276:680–683.

Thierstein, H.R., Geitzenauer, K., Molfino, B., and Shackleton, N.J., 1977. Global synchroneity of late Quaternary coccolith datum levels: validation by oxygen isotopes. *Geology*, 5:400–404.

Thunell, R.C., and Williams, D.F., 1989. Glacial-Holocene salinity changes in the Mediterranean Sea: hydrographic and depositional effects. *Nature*, 338:493–496.

Vergnaud-Grazzini, C., Ryan, W.B.F., and Cita, M.B., 1977. Stable isotope fractionation, climatic change and episodic stagnation in the Eastern Mediterranean during the Late Quaternary. *Mar. Micropaleontol.*, 2:353–370.

Vogelsang, E., 1990. Paläo-Ozeanographie des Europäischen Nordmeeres an Hand stabiler Kohlenstoff-und Sauerstoffisotope. *Ber. Sonderforschungsber. 313, Univ. Kiel*, 23:1–136.

Volkman, J.K., Barrett, S.M., Blackburn, S.I., and Sikes, E.L., 1995. Alkenones in *Gephyrocapsa oceanica:* implications for studies of paleoclimate. *Geochim. Cosmochim. Acta*, 59:513–520.

Volkman, J.K., Eglinton, G., Corner, E.D.S., and Forsberg, T.E.V., 1980. Long-chain alkenes and alkenones in the marine coccolithophorid *Emiliania huxleyi. Phytochemistry*, 19:2619–2622.

Williams, D.F., and Thunell, R.C., 1979. Faunal and oxygen isotopic evidence for surface water salinity changes during sapropel formation in the eastern Mediterranean. *Sediment. Geol.*, 23:81–93.

Date of initial receipt: 12 May 1997
Date of acceptance: 16 February 1998
Ms 161SR-237